

Impact of QED corrections to Higgs decay into four leptons at the LHC

C. M. Carloni Calame^{ab}, M. Moretti^c, G. Montagna^{ba}, O. Nicrosini^{ab}, F. Piccinini^{ab}, A.D. Polosa^d

^aINFN, Sezione di Pavia, via A. Bassi, 6, Pavia (Italy)

^bDipartimento di Fisica Nucleare e Teorica, Università di Pavia, via A. Bassi, 6, Pavia (Italy)

^cDipartimento di Fisica, Università di Ferrara, via Saragat, 1, Ferrara (Italy)

^dINFN, Sezione di Roma, piazzale A. Moro, 2, Roma (Italy)

At the LHC a precise measurement of the Higgs boson mass (if discovered), at the level of 0.1-1%, will be possible through the channel $gg \rightarrow H \rightarrow 4l$ for a wide range of Higgs mass values. To match such an accuracy, the systematic effects induced by QED corrections need to be investigated. In the present study the calculation of $\mathcal{O}(\alpha)$ and higher order QED corrections is illustrated as well as their impact on the Higgs mass determination, once realistic event selection criteria for charged leptons and photons are considered.

1. Introduction

Assuming that the Higgs boson will be discovered at the LHC, a measurement of its mass, for a large range of values, with a relative experimental precision of 0.1-1% will be possible, by combining ATLAS and CMS measurements and for an integrated luminosity of 300 fb^{-1} per experiment [1]. To match such an accuracy, the impact of QED radiative corrections on the Higgs mass determination through the gluon-fusion process $gg \rightarrow H \rightarrow 4l$ ($4l = 4e, 4\mu, e^+e^-\mu^+\mu^-$) must be evaluated. To this end, exact $\mathcal{O}(\alpha)$ and higher-order QED corrections are calculated, as described in Sect. 2, and their effect on the Higgs mass extraction in the presence of realistic event selection criteria is evaluated, as discussed in Sect. 3. Although the electromagnetic corrections affect only the final state, the effects of the production process have to be considered, because the typical event selection applied on leptons are not Lorentz invariant. The complete process $pp \rightarrow H \rightarrow 4l(\gamma)$ has been simulated in the narrow width approximation, well justified for low Higgs masses, thus allowing to factorize the production and decay processes. The obtained preliminary results shown in Sect. 3 indicate that QED radiation effects should be carefully consid-

ered in view of the expected precision at the LHC.

2. The calculation

QED radiative corrections are calculated on top of exact tree-level matrix elements for the decay $H \rightarrow Z^{(*)}Z^{(*)} \rightarrow 4l$, which, at tree level, consists of one diagram for the final state $e^+e^-\mu^+\mu^-$ and two diagrams for equal flavour leptonic pairs (see Fig. 1).

Since the tree-level is mediated by electrically neutral Z -bosons, QED corrections can be safely calculated in a gauge invariant way as a subset of the complete electroweak corrections [2], namely neglecting W -boson exchange contributions. Two complementary approaches have been adopted: the former is based on the parton shower technique, in the realization of Ref. [3], allowing to calculate QED corrections in the leading logarithmic approximation both at $\mathcal{O}(\alpha)$ and to all orders; the latter relies upon a complete $\mathcal{O}(\alpha)$ perturbative calculation. While in the first case the correction is completely factorized over the tree-level, in the diagrammatic calculation some care has to be devoted to the treatment of the Z -boson width in the virtual and real corrections in order to safely control the infrared (IR) cancellations. As for any one-loop calculation, the

expression for the decay width, fully differential over the final state, can be written as

$$d\Gamma = (d\Gamma)_B + (d\Gamma)_V + (d\Gamma)_R, \quad (1)$$

where the subscripts stand for Born (B), Virtual (V) and Real (R) contributions. The IR divergence is regularized by means of a small photon mass λ . The real corrections are calculated analytically in soft approximation for $\lambda \leq E_\gamma \leq k_0$ (where k_0 is the soft-hard separator), and by means of exact matrix elements for $E_\gamma > k_0$, with finite fermion masses and $\lambda = 0$. The real hard photon emission diagrams (one of them is shown in Fig. 2) have been calculated analytically with FORM [4] and cross-checked with ALPHA [5]. The virtual corrections consist of vertex and self-energy diagrams (see Fig. 3), which are symbolically written in terms of Passarino-Veltman form factors [6] and evaluated numerically with LoopTools [7]. In addition, also box and pentagon diagrams are present. One example of five-point graphs is given in Fig. 4. The pentagon diagrams are reduced, with the help of FORM [4], to combinations of four-point form factors by means of the techniques introduced in Ref. [8], in order to avoid numerical instabilities due to vanishing Gram determinants. The method has already been successfully used for the calculation of the $\mathcal{O}(\alpha)$ electroweak corrections to $e^+e^- \rightarrow 4$ fermions, where also six-point functions are involved [9]. Adopting the approximation of vanishing fermion masses whenever possible in the virtual corrections and performing the calculation in the 't Hooft-Feynman gauge $\xi = 1$, the involved five-point functions are at most of rank two and therefore are free of ultraviolet divergences. An additional complication is due to the presence of the unstable Z bosons. In order to avoid singularities in the phase space, the introduction of the Z width is required, which could spoil the IR cancellation between virtual and real corrections. In fact the IR divergences, contained in the non-factorizable five-point diagrams, are cancelled by the interference between real (tree-level) radiation from different external legs. A solution is given by the ‘‘complex mass scheme’’ (introduced in Ref. [10] for lowest order processes and generalized for one-

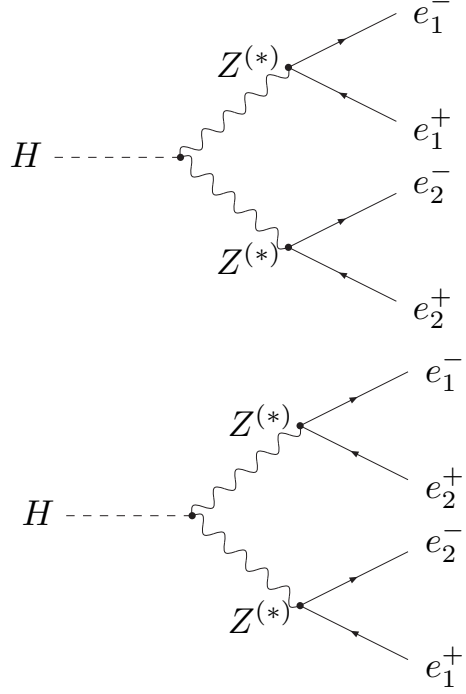


Figure 1. Born diagrams for the decay $H \rightarrow 4e$.

loop calculations in Ref. [9]), where the Z mass is shifted on the complex plane with fixed width $M_Z^2 \rightarrow M_Z^2 - i\Gamma_Z M_Z$, both in tree-level and in loop diagrams and the couplings become complex quantities, in order to respect the Ward identities. Considering that self-energies and vertex corrections, neglecting terms of $\mathcal{O}(m_f^2/Q^2)$, are already factorized over the tree-level, and that with complex M_Z the IR singularity can be factorized over the tree-level also for five-point diagrams, the $\mathcal{O}(\alpha)$ QED corrected Higgs partial width can be written as:

$$d\Gamma_{\mathcal{O}(\alpha)} = (d\Gamma)_B \times (1 + \delta_V^{\text{fact}} + \delta_V^{5-IR}) + (d\Gamma)_R + [(d\Gamma)_V^{\text{nf}} - (d\Gamma)_B \times \delta_V^{5-IR}], \quad (2)$$

where δ_V^{fact} refers to the contribution of self-energies and vertices, δ_V^{5-IR} refers to the IR scalar three-point functions representing the IR part of

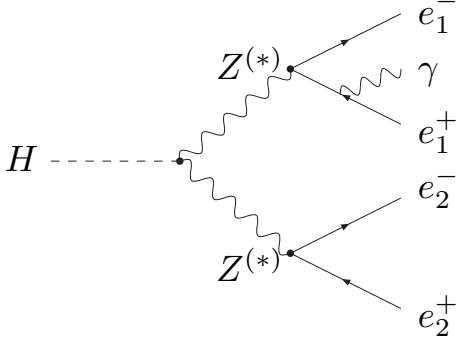


Figure 2. The real-radiation diagrams are obtained attaching a real photon leg to every final state fermion.

the five-point functions and $(d\Gamma)_V^{\text{nf}}$ is the complete contribution of the pentagon diagrams. By construction, the IR divergence has been factorized over the tree-level, thus allowing for a consistent IR cancellation with the real part $(d\Gamma)_R$, and the remainder $[(d\Gamma)_V^{\text{nf}} - (d\Gamma)_B \times \delta_V^{5-IR}]$ is free of divergence. While the numerical evaluation of two- and three-point scalar functions with complex masses is performed with `LoopTools v2.2`, the four-point scalar scalar functions is reduced to unidimensional integrals which are evaluated by means of the adaptive integration package `CUBA` [11]. With the same numerical algorithm several checks have been performed of the two- and three-point functions with complex masses obtained with `LoopTools` (which uses the formulae implemented in `FF` [12]), finding up-to-digit agreement.

In order to estimate realistically the impact of QED corrections on the Higgs mass determination, the complete production and decay process $pp \rightarrow H \rightarrow 4l + (n\gamma)$ has to be simulated, considering typical realistic event selection criteria. Since for a Higgs mass value below the real Z -pair production threshold the total width is very small compared to its mass, the narrow width approximation is adequate. In this approximation the calculation can be split in on-shell Higgs produc-

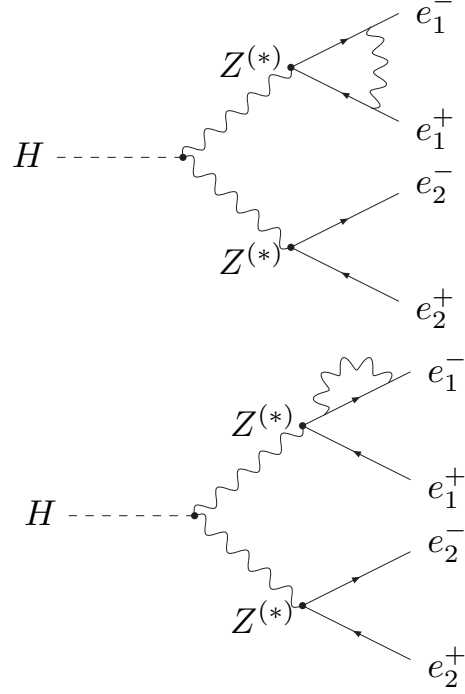


Figure 3. Vertex (upper panel) and self-energy (lower panel) diagrams contribute to the factorizable corrections.

tion \times decay, according to the following formula

$$\begin{aligned} \sigma(pp \rightarrow H \rightarrow 4l + (n\gamma)) = & \\ & \int dx_1 dx_2 f_g(x_1, \mu) f_g(x_2, \mu) \\ & \hat{\sigma}_{gg \rightarrow H} \delta(x_1 x_2 s - M_H^2) \\ & \times \int \frac{d\Gamma(H \rightarrow 4l + (n\gamma))}{\Gamma_{\text{tot}}} \Theta(\text{cuts}), \end{aligned} \quad (3)$$

where $f_g(x, \mu)$ are the gluonic parton distribution functions, $\hat{\sigma}_{gg \rightarrow H}$ is the parton level Higgs production cross section and $\Theta(\text{cuts})$ is a step function accounting for the experimental cuts.

A Monte Carlo code has been developed, based on the event generator `ALPGEN` [13] for Higgs production and an original library `H24F` for the decay into four leptons with QED radiative corrections, taking into account realistic event selections for

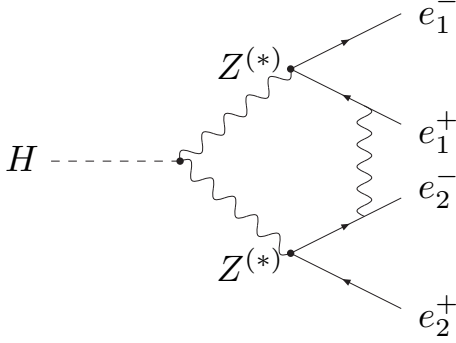


Figure 4. Example of pentagon diagram, which contributes to the non-factorizable corrections.

charged leptons and photons. The additional approximation of neglecting the Higgs transverse momentum is assumed in the present study. A more detailed investigation will be presented elsewhere.

3. Numerical results

In order to quantify the shift induced by QED corrections on the Higgs mass determination, binned χ^2 fits to the (four leptons) invariant mass distribution (see Fig. 5) have been performed, following the strategy described in detail in Ref. [14]. A reference invariant mass distribution is produced at Born level for a given Higgs mass and N invariant mass distributions are produced including radiative corrections for different Higgs masses, around the reference value (with 20 MeV spacing). N χ^2 values are then calculated, according to the following equation

$$\chi^2(m_H) = \sum_{i=\text{bins}} \frac{\left(\frac{d\sigma_{i,QED}}{\sigma_{QED}} - \frac{d\sigma_{i,Born}}{\sigma_{Born}} \right)^2}{\left[\left(\Delta \frac{d\sigma_{i,QED}}{\sigma_{QED}} \right)^2 + \left(\Delta \frac{d\sigma_{i,Born}}{\sigma_{Born}} \right)^2 \right]}, \quad (4)$$

where $d\sigma_{i,Born}/\sigma_{Born}$ and $d\sigma_{i,QED}/\sigma_{QED}$ are the Born-level and QED corrected cross sections relative to the i -th bin (normalized to the corresponding integrated cross sections). The Higgs

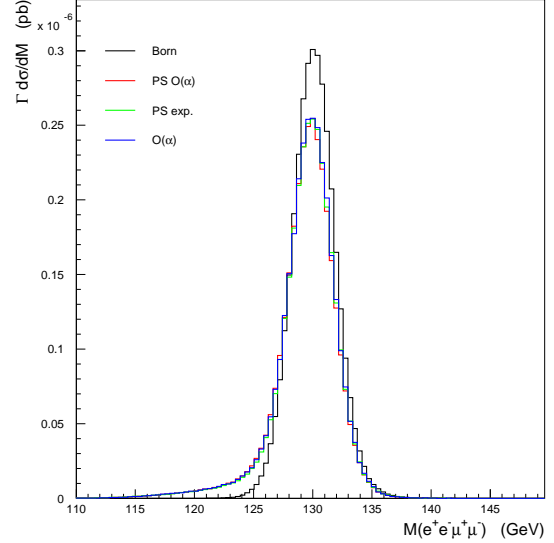


Figure 5. Higgs invariant mass in the laboratory frame for the decay $H \rightarrow e^+e^-\mu^+\mu^-$, after applying experimental cuts and momentum smearing, as obtained at tree level, with Parton Shower and with exact $\mathcal{O}(\alpha)$ corrections.

mass shift is derived from the minimum of the χ^2 distribution.

In order to be close to the experimental selection, lepton identification requirements and kinematical cuts, as well as uncertainties in the energy and transverse momentum measurements of the photons/leptons in the detector, have been implemented according to Ref. [1]. The results of this preliminary analysis are given in Tab. 1, showing the Higgs mass shifts due to $\mathcal{O}(\alpha)$ (second column) and higher-order (third column) corrections, for the three possible four lepton decays and for a Higgs mass of 130 GeV. It can be seen that the mass shift due to multiple photon radiation is, as a rule of thumb, of the order of 10% of that caused by one photon emission and, therefore, non-negligible in view of the expected precision at the LHC. Furthermore, it has been preliminarily observed that, at the present level

Table 1

The Higgs mass shifts due to $\mathcal{O}(\alpha)$ and higher-order QED corrections to $gg \rightarrow H \rightarrow 4l$ for the three different lepton final states and for a Higgs mass of 130 GeV.

Process	$ \Delta(QED)^{(\alpha)} $	$ \Delta(QED)^{(\text{exp})} - \Delta(QED)^{(\alpha)} $
$e^+e^-e^+e^-$	160 MeV	≤ 20 MeV
$e^+e^-\mu^+\mu^-$	340 MeV	≤ 50 MeV
$\mu^+\mu^-\mu^+\mu^-$	600 MeV	~ 100 MeV

of accuracy of the investigation, exact $\mathcal{O}(\alpha)$ and leading logarithmic $\mathcal{O}(\alpha)$ QED corrections induce the same mass shifts. A more detailed analysis, as well as a presentation of further numerical results, is left to a future work.

Acknowledgements

C.M. Carloni Calame is grateful to the Organizers of RADCOR05 for the pleasant and stimulating atmosphere during the conference.

REFERENCES

1. S. Asai et al., SN-ATLAS-2003-024; M. Düehrsen, ATL-PHYS-2003-030; S. Abdullin et al., CMS Note 2003/33; ATLAS Technical Design Report ATLAS-TDR 15, CERN/LHCC 99-15.
2. A. Bredenstein, A. Denner, S. Dittmaier and M.M. Weber, arXiv:[hep-ph/0604011].
3. C.M. Carloni Calame, C. Lunardini, G. Montagna, O.Nicosini and F. Piccinini, Nucl. Phys. **B584** (2000) 459; C.M. Carloni Calame, Phys. Lett., **B520** (2001) 16.
4. J.A.M. Vermaseren, arXiv:[math-ph/0010025].
5. F. Caravaglios and M. Moretti, Phys. Lett. **B358** (1995) 332.
6. G. Passarino and M.J. Veltman, Nucl. Phys. **B160** (1979) 151.
7. T. Hahn and M. Perez-Victoria, Comp. Phys. Commun. **118** (1999) 153; T. Hahn and M. Rauch, arXiv:[hep-ph/0601248].
8. A. Denner and S. Dittmaier, Nucl. Phys. **B658** (2003) 175.
9. A. Denner, S. Dittmaier, M. Roth and L.H. Wieders, Phys. Lett. **B612** (2005) 223; arXiv:[hep-ph/0505042]; A. Denner and S. Dittmaier, arXiv:[hep-ph/0509141].
10. A. Denner, S. Dittmaier, M. Roth and D. Wackeroth, Nucl. Phys. **B560** (1999) 33.
11. T. Hahn, Comput. Phys. Commun. **168** (2005) 78.
12. G.J. van Oldenborgh and J.A.M. Vermaseren, Z. Phys. **C46** (1990) 425.
13. M.L. Mangano, M. Moretti, F. Piccinini, R. Pittau and A.D. Polosa, JHEP **0307** (2003) 001.
14. C.M. Carloni Calame, G. Montagna, O.Nicosini and M. Treccani, Phys. Rev. **D69** (2004) 037301; JHEP **05** (2005) 019.